Antideuterons and antihelium nuclei from annihilating dark matter

Ilias Cholis,[1,*] Tim Linden,[2,3,†] and Dan Hooper[4,5,‡]

[1]*Department of Physics, Oakland University, Rochester, Michigan 48309, USA*
[2]*Stockholm University and the Oskar Klein Centre, Stockholm 10691, Sweden*
[3]*Center for Cosmology and AstroParticle Physics (CCAPP) and Department of Physics, The Ohio State University, Columbus, Ohio 43210, USA*
[4]*Theoretical Astrophysics Group, Fermi National Accelerator Laboratory, Batavia, Illinois 60510, USA*
[5]*Department of Astronomy and Astrophysics and the Kavli Institute for Cosmological Physics (KICP), University of Chicago, Chicago, Illinois 60637, USA*

(Received 2 February 2020; revised 26 August 2020; accepted 6 October 2020; published 16 November 2020)

Recent studies of the cosmic-ray antiproton-to-proton ratio have identified an excess of ∼10–20 GeV antiprotons relative to the predictions of standard astrophysical models. Intriguingly, the properties of this excess are consistent with the same range of dark matter models that can account for the long-standing excess of γ-rays observed from the Galactic Center. Such dark matter candidates can also produce significant fluxes of antideuterium and antihelium nuclei. Here we study the production and transport of such particles, both from astrophysical processes as well as from dark matter annihilation. Importantly, in the case of *AMS-02*, we find that Alfvénic reacceleration (i.e., diffusion in momentum space) can boost the expected number of $\bar{\mathrm{d}}$ and $^3\overline{\mathrm{He}}$ events from annihilating dark matter by an order of magnitude or more. For relatively large values of the Alfvén speed, and for dark matter candidates that are capable of producing the antiproton and γ-ray excesses, we expect annihilations to produce a few antideuteron events and about one antihelium event in 6 yr of *AMS-02* data. This is particularly interesting in light of recent reports from the *AMS-02* Collaboration describing the detection of a number of antihelium candidate events.

DOI: 10.1103/PhysRevD.102.103019

Measurements of the high-energy antimatter cosmic-ray spectra provide a powerful probe of new physics, including the annihilation or decay of dark matter particles in the halo of the Milky Way [1–5]. An excess of ∼10–20 GeV cosmic-ray antiprotons [6–10] has been identified in data from *AMS-02* [11] (and *PAMELA* [12]), with characteristics that are consistent with the annihilation of ∼50–90 GeV dark matter particles with a cross section of $\langle\sigma v\rangle \simeq (1-9)\times 10^{-26}$ cm^3/s [13] (for the case of annihilations to $b\bar{b}$; for other dark matter scenarios consistent with this signal, see Refs. [13,14]). This excess is statistically significant ($>3.3\sigma$), and robust to systematic uncertainties associated with the antiproton production cross section, the propagation of cosmic rays through the interstellar medium (ISM), and the time-, charge- and energy-dependent effects of solar modulation [13,15] (see, however, Refs. [16,17]). Intriguingly, the range of dark matter models favored by the antiproton data is also consistent with that required to explain the γ-ray excess observed from the direction of the Galactic Center [18–24].

In 2015, two groups analyzed small-scale power in the γ-ray data and argued that the γ-ray excess is likely generated by a large population of point sources (such as millisecond pulsars) [25,26]. Recent work, however, has shown the interpretation of these results to be problematic [27,28]. Reference [27] demonstrated that one class of algorithms is systematically biased towards pulsar models and is unable to recover true dark matter signals that are injected into the data (in stark contrast to a recent study limited to mock data [29]). Reference [28] has gone farther, placing constraints on the luminosity function of any point source population that is in strong tension with millisecond pulsar models [30–34].

In addition to γ-rays and antiprotons, dark matter annihilations can produce potentially detectable fluxes of heavier antinuclei, including antideuterons and antihelium [35]. As kinematic considerations strongly suppress the production of heavy antinuclei in astrophysical processes, the detection of such particles could constitute a smoking gun for dark matter annihilation. Intriguingly, the *AMS-02* Collaboration has reported preliminary evidence of $\mathcal{O}(10)$ candidate antihelium events [36]. Such a rate would significantly exceed that predicted from standard astrophysical processes or dark matter [37,38], with no other plausible means of producing so much high-energy antihelium identified [39] (see also Refs. [40–43]). For example, while

*cholis@oakland.edu
†linden@fysik.su.se
‡dhooper@fnal.gov

several groups have found that the uncertainties associated with the antinuclei production cross sections could substantially increase the number of antihelium events from dark matter annihilations [37,38], these rates still lie well below those required to explain the preliminary results from *AMS-02*.

In this paper, we investigate how variations in the cosmic-ray transport model could impact the local spectrum of antideuterium and antihelium. Most significantly, we find that diffusive reacceleration (also known as Alfvénic reacceleration or diffusion in momentum space) could dramatically increase the number of antideuterium and antihelium events predicted to be observed by *AMS-02* in annihilating dark matter scenarios. This effect is more pronounced for antihelium than for antideuterium, helping to explain the unexpectedly large number of antihelium candidate events. In models where the dark matter's mass, annihilation cross section and final state are chosen to fit the antiproton and γ-ray excesses, and for a large Alfvén speed of $v_A \sim 60$ km/s, we expect *AMS-02* to detect roughly one $^3\overline{\mathrm{He}}$ event and a few $\bar{\mathrm{d}}$ events (in 6 yr of data).

Throughout this study, we will consider two mechanisms for the production of cosmic-ray antiprotons, antideuterons and antihelium nuclei. First, antimatter can be produced through the collisions of primary cosmic rays with interstellar gas. The flux and spectrum of this contribution depend on the primary cosmic-ray spectrum and on the average quantity of gas that the cosmic rays encounter before escaping the Milky Way.[1] Second, antimatter can be produced through the annihilation of dark matter particles, with a spectrum that depends on the distribution of dark matter, as well as on the characteristics of the dark matter candidate itself. For this case, we adopt an Navarro-Frenk-White (NFW) profile [46] with a local density of 0.4 GeV/cm^3 [47,48] and a scale radius of 20 kpc. In both cases, we calculate the spectrum of antinuclei that is injected into the ISM using a "coalescence" model [49], in which two antinucleons are predicted to fuse into a common nucleus if the difference between their relative momenta is smaller than the coalescence momentum, p_0 (for details, see Appendix A).

To model the transport of cosmic rays through the ISM, we use the publicly available code GALPROP v56 [50,51], which accounts for the effects of cosmic-ray diffusion, convection, diffusive reacceleration and fragmentation, as well as energy losses from ionization, Coulomb interactions, synchrotron, bremsstrahlung and inverse Compton scattering emission.[2] This transport model assumes diffusion to be isotropic and homogeneous within a cylindrical zone centered at the Galactic Center. We adopt a diffusion coefficient of the form $D_{xx}(R) = \beta D_0 (R/4GV)^{\delta}$, where $\beta \equiv v/c$ and $\delta \sim 0.3$–0.5 [52] is the diffusion index associated with magnetohydrodynamic turbulence in the ISM. We additionally allow particles to be propelled out of the plane by convective winds, with a speed that is zero at the plane and that increases at larger heights as

$$v_c = \frac{dv_c}{d|z|}|z|. \tag{1}$$

The spatial diffusion of cosmic rays is the result of scattering on magnetic turbulence. In addition, cosmic rays experience diffusive reacceleration (or Alfvénic reacceleration) due to the resonant interaction of charged particles of a given gyroradius with the corresponding Alfén modes of the turbulent medium. This is manifest as diffusion in momentum space with the following coefficient [53]:

$$D_{pp} \propto \frac{R^2 v_A^2}{D_{xx}(R)}, \tag{2}$$

where the Alfvén speed, v_A, is the speed that hydromagnetic waves propagate through the ISM plasma.

We begin our analysis using ISM Models I, II, and III from Ref. [13], and then consider alterations to these reference scenarios. While diffusion, convection, and diffusive reacceleration each play significant roles in determining the spectra of cosmic-ray antinuclei, we find that the very strong constraints on the diffusion coefficient (from measurements of the B/C ratio and Voyager measurements of the low-energy cosmic-ray flux), strongly constrain the combined values of D_0 and δ. Instead, the current data allow for much larger variations in the properties of convection and diffusive reacceleration, making them the dominant sources of uncertainty in predicting the resulting cosmic-ray antinuclei spectra. To include the uncertainties associated with the effects of solar modulation, we use the model of Ref. [44]. Our approach is the same as that adopted in Refs. [13,44,45], accounting for measurements of the magnitude of the heliospheric magnetic field from *ACE* [54] and its morphology from the Wilcox Solar Observatory [55].

In Fig. 1, we plot the spectrum of $\bar{\mathrm{p}}$, $\bar{\mathrm{d}}$, $^3\overline{\mathrm{He}}$ and $^4\overline{\mathrm{He}}$ from standard astrophysical production, and compare this to the contributions predicted from annihilating dark matter. In particular, we consider a dark matter model that is capable of producing the observed features of the antiproton and γ-ray excesses ($m_\chi = 67$ GeV, $\sigma v = 2 \times 10^{-26}$ cm^3/s and $\chi\chi \to b\bar{b}$) [9,10,13,23,56]. The solid curves represent the

[1]We adopt a spectrum and spatial distribution of injected primary cosmic rays that provides a good fit to the measured primary-to-secondary ratios. More specifically, the injected spectra are described by a broken power-law in rigidity with an index of 1.9 (2.38–2.45), below (above) a break of 11.7 GV for all cosmic-ray species [13,44,45].

[2]We emphasize that throughout this study antimatter nuclei fragmentations are included. Ignoring fragmentations would result in enhancing the $\bar{\mathrm{d}}$ and $^3\overline{\mathrm{He}}$ predicted fluxes from 30% at $\lesssim$GeV/n in E_{kin} to a factor of 2 at $E_{\mathrm{kin}} = 10$ GeV/n; increasing the respective events by a factor of $\simeq$2.

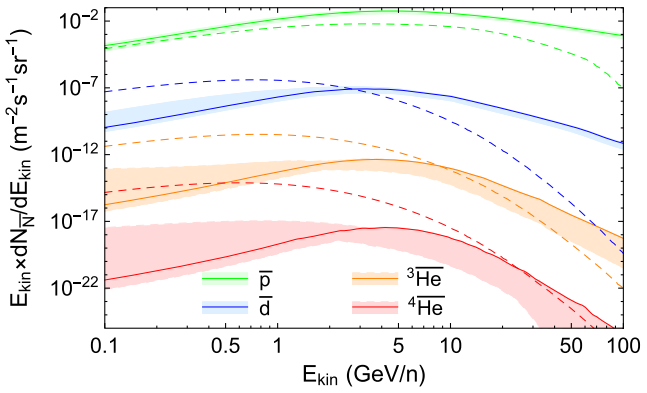

FIG. 1. The spectrum of cosmic-ray $\bar{p}$ (green), $\bar{d}$ (blue), $^3\overline{He}$ (orange) and $^4\overline{He}$ (red) from standard astrophysical production (solid curves), along with the uncertainty associated with this prediction (bands), for the case of ISM Model I. The dashed curves are the central prediction for the antinuclei spectra from an annihilating dark matter model that can produce the antiproton and γ-ray excesses ($m_\chi = 67$ GeV, $\sigma v = 2 \times 10^{-26}$ cm^3/s, $\chi\chi \to b\bar{b}$). Note that diffusive reacceleration can lead to nonzero antinuclei fluxes from annihilating dark matter well above the maximum injected energy of such particles.

central value of the astrophysical predictions, while the surrounding bands reflect the total uncertainty, adopting the assumptions described in Appendix A (and adopting $p_0 = 261$ MeV for $^3\overline{He}$ and $^4\overline{He}$). The dashed lines depict our central prediction from the selected annihilating dark matter model.

The contribution from dark matter dominates the spectrum of antinuclei at low energies, as dark matter annihilation occurs in the laboratory frame, while astrophysical secondary production necessarily occurs in a boosted frame. Furthermore, the dark matter contribution becomes increasingly dominant for more massive antinuclei, due to the increasing kinematic suppression of secondary production mechanisms. In Table I, we show the number of $\bar{d}$, $^3\overline{He}$ and $^4\overline{He}$ events that we predict *AMS-02* will observe with 6 yr of data, from astrophysical secondary production and from dark matter annihilation. To calculate these rates, we combine the spectra shown in Fig. 1 with the reported sensitivity of *AMS-02* [57].

We emphasize two aspects of our results. First, the rate of antinuclei events from dark matter consistently exceeds that predicted from astrophysical production. Second, the number of events from secondary production is not significantly affected by the choice of ISM Model, while the dark matter flux can change by several orders of magnitude in different ISM Models. This is due to the significant effect of cosmic-ray propagation on the spectrum of antinuclei from dark matter annihilation. As we will show, this is the key result of this paper.

In Fig. 2, we illustrate the impact of diffusive reacceleration and convection on the number of antinuclei events from dark matter predicted to be observed by *AMS-02*. Here, we have fixed all of the propagation parameters to those of ISM Model I, with the exception of the Alfvén speed and convection velocity, which are varied in the left and right frames, respectively (the default values in ISM Model I are $v_A = 24$ km/s and $dv_c/d|z| = 1$ km/s/kpc). The shaded bands in this figure represent the uncertainties associated with coalescence and solar modulation.

While the predicted number of antideuteron events is roughly flat for values of v_A above ~20 km/s, the number of antihelium events is highly sensitive to this quantity. For large values of v_A, *AMS-02* could detect $O(1)$ $^3\overline{He}$ event over 6 yr of operation. In contrast, increasing the convection velocity has the effect of suppressing the number of antideuteron and antihelium events observed by *AMS-02*.

To understand the dependence of these event rates on the Alfvén speed, it is important to appreciate that *AMS-02* is sensitive to antinuclei only across a limited range of energies. As illustrated in Fig. 3, *AMS-02* reports sensitive to antideuterons only in the ranges of 0.18–0.72 and 2.2–4.6 GeV/n. As dark matter annihilations are predicted to produces a large flux antideuterons below this range of energies, even a modest amount of diffusive reacceleration can quite dramatically increase the rate at which such particles are ultimately detected by *AMS-02*. The rate of $^3\overline{He}$ events is even more sensitive to the Alfvén speed due to the higher energy range across which *AMS-02* can detect and identify such particles [58]. Convective winds instead, reduce the local flux of antinuclei. This is particularly important at low energies, where diffusion is less efficient.

TABLE I. The number of $\bar{d}$, $^3\overline{He}$ and $^4\overline{He}$ events that *AMS-02* is expected to observe with 6 yr of data from astrophysical secondary production ("Astro") and from dark matter annihilation. For the case of dark matter, we adopt a model of $m_\chi = 67$ GeV, $\sigma v = 2 \times 10^{-26}$ cm^3/s, $\chi\chi \to b\bar{b}$, and show rates using three ISM transport models (Models I, II and III of Ref. [13]). For the case of astrophysical secondary production we have marginalized over these three models. The ranges shown include the uncertainties associated with in the coalescence momenta, the proton-proton cross section, and the effects of solar modulation.

	Astro	DM (I)	DM (II)	DM (III)
$\bar{d}$	0.02–0.1	0.6–3.0	0.4–2	0.3–1.5
$^3\overline{He}$	$(0.3–3) \times 10^{-3}$	0.01–0.1	$(0.6–6) \times 10^{-2}$	$(0.5–5) \times 10^{-2}$
$^4\overline{He}$	$(0.06–6) \times 10^{-9}$	$(0.2–5) \times 10^{-4}$	$(0.8–15) \times 10^{-6}$	$(0.6–12) \times 10^{-6}$

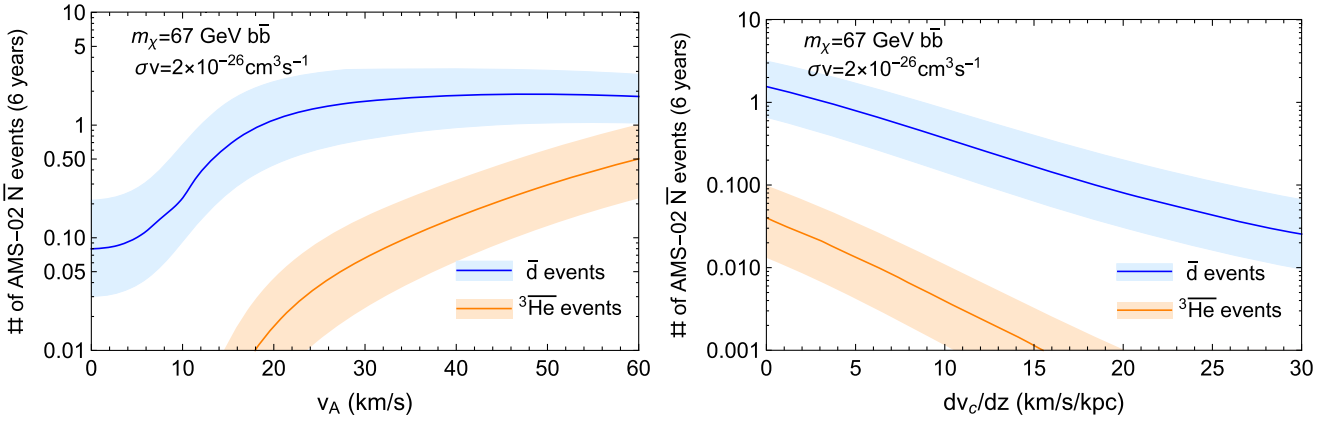

FIG. 2. The number of $\bar{d}$ and $^3\overline{He}$ events predicted to be observed by *AMS-02* in 6 yr of data from annihilating dark matter ($m_\chi = 67$ GeV, $\sigma v = 2 \times 10^{-26}$ cm^3/s, $\chi\chi \to b\bar{b}$). In the left (right) frame, we vary the Alfvén speed (convection velocity gradient) while keeping all of the other propagation parameters set to those of ISM Model I [13]. The bands represent the uncertainties associated with the coalescence momentum and solar modulation.

Relative to that from annihilating dark matter, the rate of antinuclei events from astrophysical secondary production is far less sensitive to the values of the Alfvén speed or convection velocity. This is due to the kinematics associated with the two processes. In particular, the secondary production of $\bar{d}$ ($^3\overline{He}$) requires the primary cosmic ray to have a kinetic energy in excess of 17 m_p (31 m_p), and thus such particles are invariably highly boosted [35]. In contrast, dark matter annihilations occur in the center-of-mass frame.

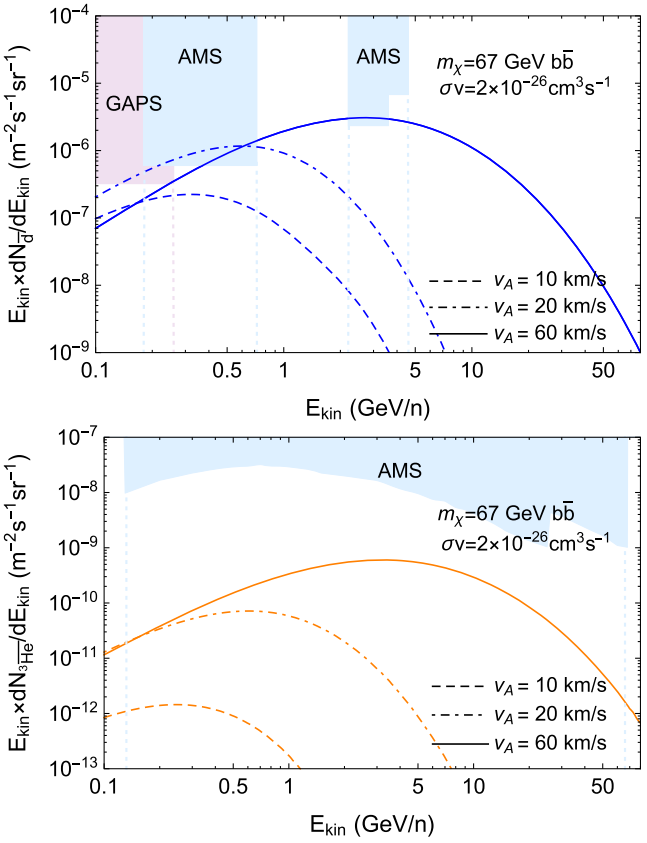

FIG. 3. The spectrum of cosmic-ray antideuterons and antihelium nuclei from annihilating dark matter ($m_\chi = 67$ GeV, $\sigma v = 2 \times 10^{-26}$ cm^3/s, $\chi\chi \to b\bar{b}$), for three values of the Alfvén speed. This is compared to the sensitivities of the *AMS-02* [57] (blue) and GAPS [40] (purple) experiments.

Finally, we show in Fig. 4 the regions of the dark matter parameter space in which one would expect *AMS-02* to observe one $\bar{d}$ or one $^3\overline{He}$ event, and compare this to the regions that are consistent with the observed characteristics of the antiproton and γ-ray excesses, as well as the constraints derived from gamma-ray observations of dwarf galaxies [59] and the cosmic microwave background (CMB) [60]. For the parameter values considered (ISM Model I, $v_A = 60$ km/s, $p_0 = 160$ MeV), the regions favored by the observed excesses are predicted to result in roughly ∼1 $^3\overline{He}$ event and a few $\bar{d}$ events (in 6 yr of *AMS-02* data).

In summary, even after accounting for the uncertainties associated with the proton-proton cross section, the coalescence model, the injection into and transport through the ISM, and solar modulation, we find that astrophysical secondary production cannot produce a flux of antideuterons or antihelium nuclei that would be detectable by *AMS-02*. However, dark matter annihilating to hadronic final states (or to particles that decay hadronically [14]) could potentially produce a detectable flux of such particles. We emphasize that the rate of antinuclei events from dark matter annihilations depends very sensitively on the impact of diffusive reacceleration. In particular, we have demonstrated that by increasing the Alfvén speed from 10 to 60 km/s, for example, one could increase the predicted rate of antideuteron (antihelium) events from dark matter by more than an order of magnitude (2 orders of magnitude); see Fig. 2. To our knowledge, this fact has not been previously discussed in the literature.

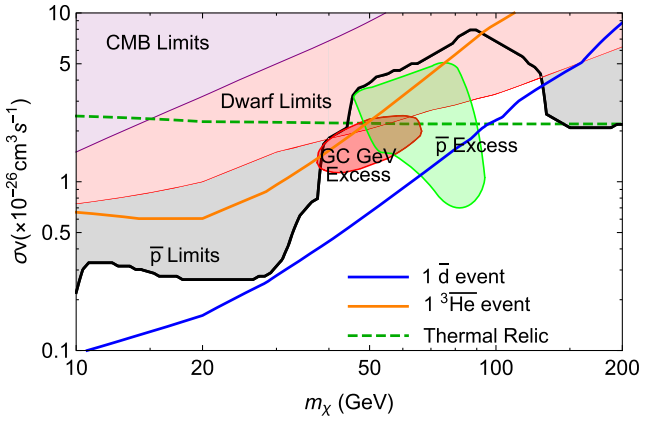

FIG. 4. The regions of the dark matter parameter space (for the case of $\chi\chi \to b\bar{b}$) in which one would expect *AMS-02* to observe one $\bar{\mathrm{d}}$ or one $^3\overline{\mathrm{He}}$ event in 6 yr of data. Also shown are the regions that are consistent with the observed characteristics of the antiproton [13] and γ-ray [23] excesses, as well as the constraints derived from gamma-ray observations of dwarf galaxies [59], the cosmic microwave background (CMB) [60], and the cosmic-ray antiproton-to-proton ratio [13]. Here we have adopted a coalescence momentum of $p_0 = 160$ MeV, an Alfvén speed of $v_A = 60$ km/s, and ISM Model I.

The *AMS-02* Collaboration has recently reported the tentative observation of $\mathcal{O}(10)$ candidate $^3\overline{\mathrm{He}}$ events. Needless to say, this would be an incredibly exciting result if confirmed. While our model does not naively predict such a large number of $^3\overline{\mathrm{He}}$ events, the results presented here provide an important path forward toward understanding the uncertainties that must be at play in order to account for such a large signal. More specifically, our results indicate that if dark matter is responsible for producing more than a few $^3\overline{\mathrm{He}}$ events at *AMS-02*, the coalescence momentum for antihelium must significantly exceed the constraints presented in Ref. [61], and the average Alfvén speed must significantly exceed the best-fit values of standard GALPROP models (∼20 km/s). Notably, both of these quantities can be independently probed with new data (the degeneracy between the Alfvén speed and other propagation parameters will be the subject of future work). We note that this antinuclei flux is produced at regions of high dark matter density as the inner two kiloparsecs of the Milky Way or close-by subshalos. Thus, the values of high Alfvén speed do not need to represent the entirety of the ISM just the regions with high dark matter density.[3]

Lastly, the results presented here are consistent with the possibility that both the γ-ray excess from the Galactic Center [18–24] and the cosmic-ray antiproton-excess [9,13,15] could arise from a 50–80 GeV dark matter particle annihilating with a cross section near that predicted for a thermal relic, $\langle\sigma v\rangle \sim 2 \times 10^{-26}$ cm^3/s. Furthermore, in such a scenario, we expect *AMS-02* to observe up to roughly one antihelium event and a few antideuterons, depending on the values of the Alfvén speed and convection velocity. Moreover, such a model remains consistent with current constraints from dwarf spheroidal galaxies and the cosmic microwave background.

ACKNOWLEDGEMENTS

We would like to thank Simeon Bird and Marc Kamionkowski for valuable discussions, Peter Reimitz for assistance with the HERWIG code and Michael Korsmeier and Martin Winkler for valuable comments on the manuscript. I. C. is partially supported by the Oakland University Research Committee Faculty Fellowship Award. T. L. is partially supported by the Swedish Research Council under Contract No. 2019-05135, the Swedish National Space Agency under Contract No. 117/19 and the European Research Council under Grant No. 742104. D. H. is supported by the US Department of Energy under contract DE-FG02-13ER41958. Fermilab is operated by Fermi Research Alliance, LLC, under Contract No. DE- AC02-07CH11359 with the U.S. Department of Energy. Reference No. FERMILAB-PUB-20-021-A.

APPENDIX A: THE INJECTED SPECTRUM OF COSMIC-RAY ANTI-NUCLEI

To calculate the spectrum of antinuclei produced through dark matter annihilation, we first determine the spectrum of antinucleons using PPPC4DMID [66].[4] We then model the relevant nuclear physics involved, employing the so-called "coalescence" model [49], in which two antiprotons or antineutrons combine to form a common nucleus if the difference between their relative momenta is smaller than the coalescence momentum, p_0. We further simplify this calculation by assuming that the production of a second antinucleon is independent of the production probability of the first (that is, there is no correlation between the flux or momentum of the particles in individual collisions) [42]. Simulations of correlated antiparticle production in Monte Carlo event generators have found that this

[3]Ref. [62], placed constraints on the maximum averaged Alfvén speed (as low as 30 km/s) in the Milky Way's ISM based on cosmic-ray power requirements. However, those are sensitive to the exact ISM diffusion assumptions. Also Refs. [63–65] have placed constraints from the associated synchrotron emission of cosmic-ray electrons the strength of which depend on the B-field morphology and magnitude.

[4]In comparing the output of PPPC4DMID to that obtained using the Monte Carlo event generators PYTHIA [67] and HERWIG [68], we find that an order one difference can in some cases arise in the γ-ray and antiproton spectra, resulting from variations in the underlying hadronization and fragmentation algorithms [69]. More specifically, we find that HERWIG typically predicts lower fluxes of antiprotons, antideuterons, and antihelium nuclei than either PYTHIA or PPPC4DMID.

assumption is adequate in the $m_\chi \sim 50$–100 GeV range considered here [70]. Under this assumption, the differential cross sections for $\bar{\mathrm{d}}$, $^3\overline{\mathrm{He}}$ and $^4\overline{\mathrm{He}}$ production can be written as

$$E_{A,Z}\frac{d^3\sigma_{A,Z}}{dp_{A,Z}^3} = \frac{m_{A,Z}}{m_p^{|Z|}m_n^{A-|Z|}}\left(\frac{1}{\sigma_{pp}}\frac{4\pi}{3}\frac{p_0^3}{8}\right)^{A-1} \times \left(E_{\bar{p}}\frac{d^3\sigma_{\bar{p}}}{dp_{\bar{p}}^3}\right)^{|Z|}\left(E_{\bar{n}}\frac{d^3\sigma_{\bar{n}}}{dp_{\bar{n}}^3}\right)^{A-|Z|}, \quad \text{(A1)}$$

where σ_{pp} is the total proton-proton cross section and A and Z are the mass and atomic number of the species, respectively. For the case of $dN_{\bar{p}}/dE_{\bar{p}} = dN_{\bar{n}}/dE_{\bar{n}}$, this leads to the following differential spectra of antinuclei:

$$\begin{aligned}
\frac{dN_{\bar{d}}}{dE_{\bar{d}}} &= \frac{m_{\bar{d}}}{m_p m_n}\frac{4}{3}\frac{p_0^3}{8p_{\bar{d}}}\frac{dN_{\bar{p}}}{dE_{\bar{p}}}\frac{dN_{\bar{n}}}{dE_{\bar{n}}},\\
\frac{dN_{^3\overline{\mathrm{He}}}}{dE_{^3\overline{\mathrm{He}}}} &= \frac{m_{^3\overline{\mathrm{He}}}}{m_p^2 m_n}3\left(\frac{p_0^3}{8p_{^3\overline{\mathrm{He}}}}\right)^2\left(\frac{dN_{\bar{p}}}{dE_{\bar{p}}}\right)^2\frac{dN_{\bar{n}}}{dE_{\bar{n}}},\\
\frac{dN_{^4\overline{\mathrm{He}}}}{dE_{^4\overline{\mathrm{He}}}} &= \frac{m_{^4\overline{\mathrm{He}}}}{m_p^2 m_n^2}\frac{4^4}{3^3}\left(\frac{p_0^3}{8p_{^4\overline{\mathrm{He}}}}\right)^3\left(\frac{dN_{\bar{p}}}{dE_{\bar{p}}}\right)^2\left(\frac{dN_{\bar{n}}}{dE_{\bar{n}}}\right)^2. \quad \text{(A2)}
\end{aligned}$$

We evaluate the fluxes of secondary $\bar{\mathrm{d}}$, $^3\overline{\mathrm{He}}$ and $^4\overline{\mathrm{He}}$ for primary cosmic ray species as heavy as silicon, and include interactions with both hydrogen and helium gas. We note that $^3\overline{\mathrm{He}}$ can be formed both directly, or through the decay of antitritium at an equivalent rate. In all cases, we vary the normalization of the total Milky Way gas density from default GALPROP values by up to $\pm 10\%$.

Increasing the value of the coalescence momentum, p_0, opens the phase space and leads to larger fluxes of antinuclei. This effect is particularly important in the case of heavier antinuclei. The impact of the uncertainty in p_0 on the local ratio of $^3\overline{\mathrm{He}}$ and $\bar{\mathrm{d}}$ has been explored in Refs. [37,38,42]. Here, we follow Ref. [42], which includes separate treatments of p_0 from dark matter and astrophysical interactions. For antinuclei from dark matter annihilation, we adopt $p_0 = 160 \pm 19$ MeV, based on measurements at e^+e^- colliders [61], while for secondary production, we use the range of $p_0 = 208$–262 MeV for $\bar{\mathrm{d}}$ and $p_0 = 218$–261 MeV for $^3\overline{\mathrm{He}}$, based on measurements of proton-proton collisions [71]. There are no existing measurements for the case of $^4\overline{\mathrm{He}}$ production, so we adopt the same p_0 range as we did for $^3\overline{\mathrm{He}}$.

In addition to the uncertainty associated with the value of p_0, the inclusive antiproton and antineutron production cross sections in proton-proton collisions are uncertain at a level between $\pm 10\%$ and $\pm 50\%$ for cosmic-ray daughter particles with rigidities between 0.5 and 500 GV. Combining these factors leads to an overall uncertainty in the antideuteron production cross section that is a factor of $\sim$2.5 at 10 GeV and $\sim$8 above 200 GeV. The uncertainties are even larger for $^3\overline{\mathrm{He}}$ and $^4\overline{\mathrm{He}}$.[5]

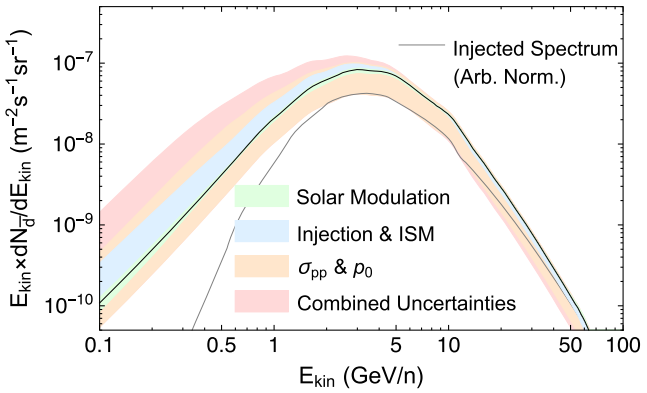

FIG. 5. The spectrum of cosmic-ray antideuterons predicted from standard astrophysical production, along with the various uncertainties associated with this prediction. The black curve is our central prediction for the case of ISM Model I and the colored bands represent the uncertainties associated with solar modulation (green), the injection and ISM transport model (blue) and the antiproton production cross section and coalesence momentum (orange). The red band depicts the total uncertainty associated with the combination of these factors.

In Fig. 5, we show the spectrum of cosmic-ray antideuterons predicted from standard astrophysical production, along with the various uncertainties associated with this prediction. The black curve represents our central prediction for the case of ISM Model I (taking $\chi\chi \to b\bar{b}$), and adopting the antiproton production cross section of Ref. [72], a coalescence momentum of $p_0 = 262$ MeV, and the best-fit solar modulation model of Ref. [44]. The colored bands represent the uncertainties associated with the effects of solar modulation (green) [44], the injection and ISM transport model (blue) [13], and the antiproton production cross section and coalesence momentum (orange) [51,71]. The larger red band depicts the total uncertainty associated with the combination of these factors.

APPENDIX B: DEPENDENCE ON THE DARK MATTER MASS

In the main body of this paper, we focused on the case of dark matter particles with a mass of 67 GeV. In this section, we show results for two other values of this quantity, 50 and 90 GeV. Changing the dark matter mass can affect the observed number of $\bar{\mathrm{d}}$ and $^3\overline{\mathrm{He}}$ events, as shown in Fig. 6. In the mass range of 20–100 GeV, lighter dark matter particles produce larger numbers of $\bar{\mathrm{d}}$ and $^3\overline{\mathrm{He}}$ events at *AMS-02* (for

[5]Annihilations of antinuclei provide only a very small correction, at one part in $\sim 10^3$. Additionally, the tertiary components of $\bar{\mathrm{d}}$, $^3\overline{\mathrm{He}}$ and $^4\overline{\mathrm{He}}$ can be absorbed into the uncertainties associated with propagation through the ISM.

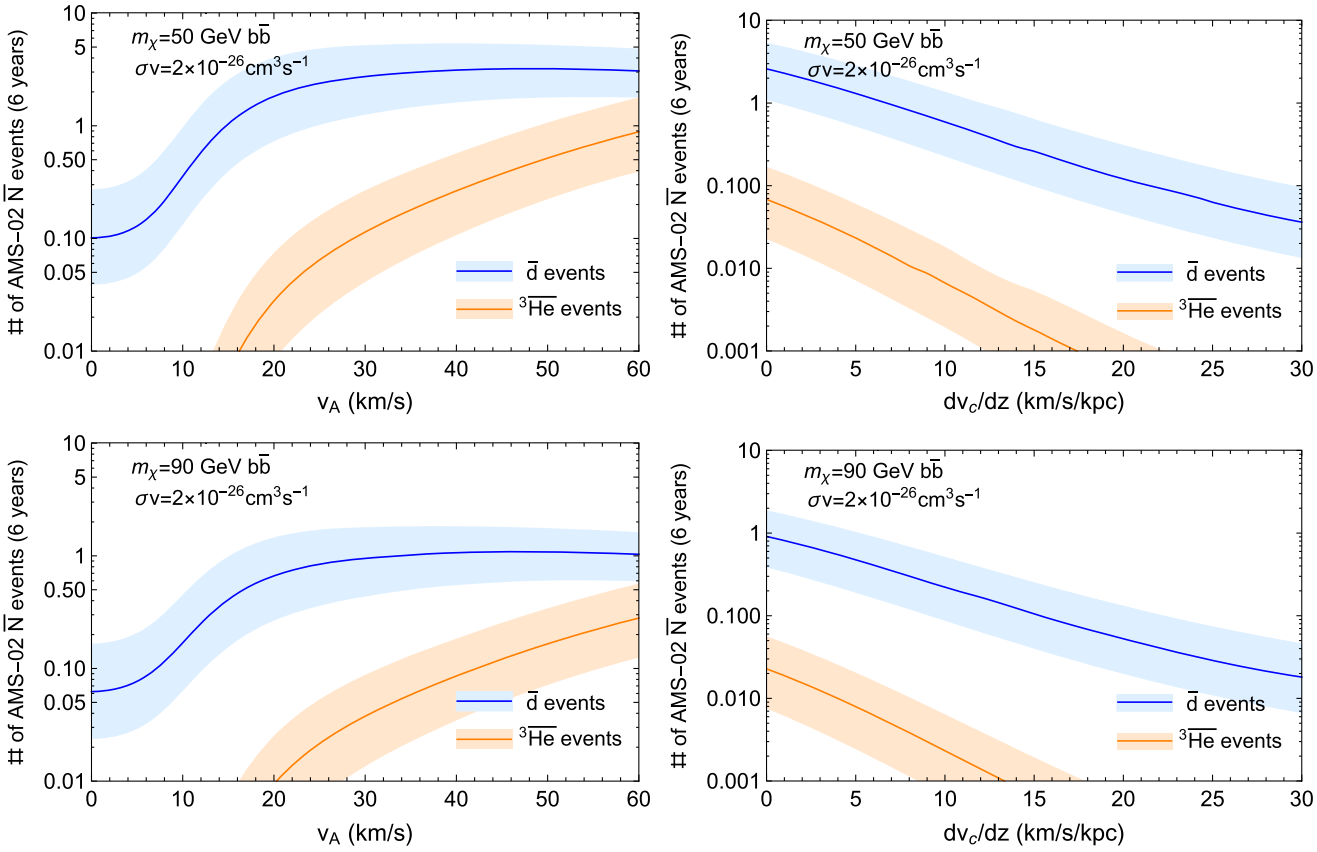

FIG. 6. As in Fig. 2, but for dark matter particles with a mass of 50 GeV (top) or 90 GeV (bottom), and that annihilate to $b\bar{b}$ with a cross section of $\sigma v = 2 \times 10^{-26}$ cm^3/s.

a given value of $\langle \sigma v \rangle$) due to their higher annihilation rate in the halo of the Milky Way.

APPENDIX C: PROSPECTS FOR THE GAPS EXPERIMENT

Here, we discuss the additional information that could be provided by the General AntiParticle Spectrometer (GAPS) experiment [40,73]. In order to illustrate the complementary of GAPS and *AMS-02*, we plot in Fig. 7 the predicted ratio of antideuteron events at GAPS to that at *AMS-02*, each as a function of the Alfvén speed or convection velocity. In calculating these results, we have assumed 35 days and 6 yr of data for GAPS and *AMS-02*, respectively. For low values of v_A or high values of dv_c/dz, GAPS is expected to observed a larger number of antideuteron events than *AMS-02*.

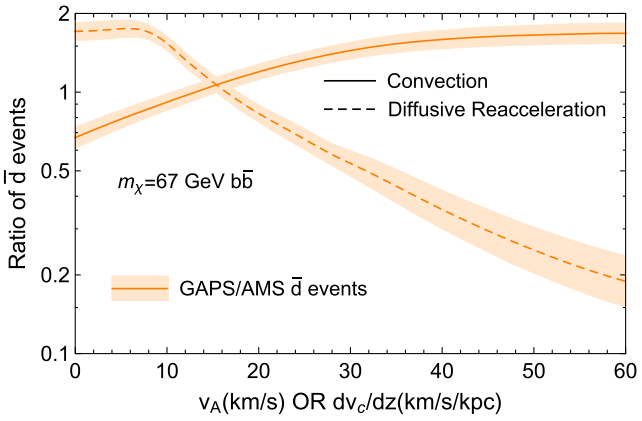

FIG. 7. The expected ratio of antideuteron events at GAPS to at *AMS-02*, as a function of the Alfvén speed and convection velocity. We assume 35 days and 6 yr of data from GAPS and *AMS-02*, respectively.

[1] L. Bergstrom, J. Edsjo, and P. Ullio, Cosmic anti-protons as a probe for supersymmetric dark matter? Astrophys. J. **526**, 215 (1999).

[2] D. Hooper, J. E. Taylor, and J. Silk, Can supersymmetry naturally explain the positron excess? Phys. Rev. D **69**, 103509 (2004).

[3] S. Profumo and P. Ullio, The role of antimatter searches in the hunt for supersymmetric dark matter, J. Cosmol. Astropart. Phys. 07 (2004) 006.

[4] T. Bringmann and P. Salati, The galactic antiproton spectrum at high energies: Background expectation vs exotic contributions, Phys. Rev. D **75**, 083006 (2007).

[5] M. Pato, D. Hooper, and M. Simet, Pinpointing cosmic ray propagation with the AMS-02 Experiment, J. Cosmol. Astropart. Phys. 06 (2010) 022.

[6] D. Hooper, T. Linden, and P. Mertsch, What Does The PAMELA Antiproton Spectrum Tell Us About Dark Matter? J. Cosmol. Astropart. Phys. 03 (2015) 021.

[7] M. Cirelli, D. Gaggero, G. Giesen, M. Taoso, and A. Urbano, Antiproton constraints on the GeV gamma-ray excess: A comprehensive analysis, J. Cosmol. Astropart. Phys. 12 (2014) 045.

[8] T. Bringmann, M. Vollmann, and C. Weniger, Updated cosmic-ray and radio constraints on light dark matter: Implications for the GeV gamma-ray excess at the Galactic center, Phys. Rev. D **90**, 123001 (2014).

[9] A. Cuoco, M. Krämer, and M. Korsmeier, Novel Dark Matter Constraints from Antiprotons in Light of AMS-02, Phys. Rev. Lett. **118**, 191102 (2017).

[10] M.-Y. Cui, Q. Yuan, Y.-L. Sming Tsai, and Y.-Z. Fan, Possible Dark Matter Annihilation Signal in the AMS-02 Antiproton Data, Phys. Rev. Lett. **118**, 191101 (2017).

[11] M. Aguilar *et al.* (AMS Collaboration), Antiproton Flux, Antiproton-to-Proton Flux Ratio, and Properties of Elementary Particle Fluxes in Primary Cosmic Rays Measured with the Alpha Magnetic Spectrometer on the International Space Station, Phys. Rev. Lett. **117**, 091103 (2016).

[12] O. Adriani *et al.* (PAMELA), PAMELA Results on the Cosmic-Ray Antiproton Flux from 60 MeV to 180 GeV in Kinetic Energy, Phys. Rev. Lett. **105**, 121101 (2010).

[13] I. Cholis, T. Linden, and D. Hooper, A robust excess in the cosmic-ray antiproton spectrum: Implications for annihilating dark matter, Phys. Rev. D **99**, 103026 (2019).

[14] D. Hooper, R. K. Leane, Y.-D. Tsai, S. Wegsman, and S. J. Witte, A systematic study of hidden sector dark matter: Application to the gamma-ray and antiproton excesses, J. High Energy Phys. 07 (2020) 163.

[15] A. Cuoco, J. Heisig, L. Klamt, M. Korsmeier, and M. Krämer, Scrutinizing the evidence for dark matter in cosmic-ray antiprotons, Phys. Rev. D **99**, 103014 (2019).

[16] A. Reinert and M. W. Winkler, A precision search for WIMPs with charged cosmic rays, J. Cosmol. Astropart. Phys. 01 (2018) 055.

[17] M. Boudaud, Y. Génolini, L. Derome, J. Lavalle, D. Maurin, P. Salati, and P. D. Serpico, AMS-02 antiprotons are consistent with a secondary astrophysical origin, Comput. Phys. Commun. **247**, 106942 (2020).

[18] D. Hooper and L. Goodenough, Dark matter annihilation in the galactic center as seen by the fermi gamma ray space telescope, Phys. Lett. B **697**, 412 (2011).

[19] D. Hooper and T. Linden, On the origin of the gamma rays from the galactic center, Phys. Rev. D **84**, 123005 (2011),

[20] K. N. Abazajian and M. Kaplinghat, Detection of a gamma-ray source in the galactic center consistent with extended emission from dark matter annihilation and concentrated astrophysical emission, Phys. Rev. D **86**, 083511 (2012); Erratum, Phys. Rev. D **87**, 129902 (2013).

[21] C. Gordon and O. Macias, Dark matter and pulsar model constraints from galactic center fermi-lat gamma ray observations, Phys. Rev. D **88**, 083521 (2013); Erratum, Phys. Rev. D **89**, 049901 (2014).

[22] T. Daylan, D. P. Finkbeiner, D. Hooper, T. Linden, S. K. N. Portillo, N. L. Rodd, and T. R. Slatyer, The characterization of the gamma-ray signal from the central Milky Way: A case for annihilating dark matter, Phys. Dark Universe **12**, 1 (2016).

[23] F. Calore, I. Cholis, and C. Weniger, Background model systematics for the Fermi GeV excess, J. Cosmol. Astropart. Phys. 03 (2015) 038.

[24] M. Ajello *et al.* (Fermi-LAT), Fermi-LAT observations of high-energy γ-ray emission toward the galactic center, Astrophys. J. **819**, 44 (2016).

[25] R. Bartels, S. Krishnamurthy, and C. Weniger, Strong Support for the Millisecond Pulsar Origin of the Galactic Center GeV Excess, Phys. Rev. Lett. **116**, 051102 (2016).

[26] S. K. Lee, M. Lisanti, B. R. Safdi, T. R. Slatyer, and W. Xue, Evidence for Unresolved γ-Ray Point Sources in the Inner Galaxy, Phys. Rev. Lett. **116**, 051103 (2016).

[27] R. K. Leane and T. R. Slatyer, Revival of the Dark Matter Hypothesis for the Galactic Center Gamma-Ray Excess, Phys. Rev. Lett. **123**, 241101 (2019).

[28] Y.-M. Zhong, S. D. McDermott, I. Cholis, and P. J. Fox, A New Mask for an Old Suspect: Testing the Sensitivity of the Galactic Center Excess to the Point Source Mask, Phys. Rev. Lett. **124**, 231103 (2020).

[29] L. J. Chang, S. Mishra-Sharma, M. Lisanti, M. Buschmann, N. L. Rodd, and B. R. Safdi, Characterizing the nature of the unresolved point sources in the Galactic Center: An assessment of systematic uncertainties, Phys. Rev. D **101**, 023014 (2020).

[30] I. Cholis, D. Hooper, and T. Linden, Challenges in explaining the galactic center gamma-ray excess with millisecond pulsars, J. Cosmol. Astropart. Phys. 06 (2015) 043.

[31] D. Hooper and T. Linden, The gamma-ray pulsar population of globular clusters: Implications for the GeV excess, J. Cosmol. Astropart. Phys. 08 (2016) 018.

[32] D. Hooper and G. Mohlabeng, The gamma-ray luminosity function of millisecond pulsars and implications for the GeV excess, J. Cosmol. Astropart. Phys. 03 (2016) 049.

[33] H. Ploeg, C. Gordon, R. Crocker, and O. Macias, Consistency between the luminosity function of resolved millisecond pulsars and the galactic center excess, J. Cosmol. Astropart. Phys. 08 (2017) 015.

[34] R. T. Bartels, T. D. P. Edwards, and C. Weniger, Bayesian model comparison and analysis of the Galactic disc population of gamma-ray millisecond pulsars, Mon. Not. R. Astron. Soc. **481**, 3966 (2018).

[35] F. Donato, N. Fornengo, and P. Salati, Anti-deuterons as a signature of supersymmetric dark matter, Phys. Rev. D **62**, 043003 (2000).

[36] AMS-02 Collaboration, *AMS Days at La Palma, La Palma, Canary Islands, Spain (2018)*.

[37] E. Carlson, A. Coogan, T. Linden, S. Profumo, A. Ibarra, and S. Wild, Antihelium from Dark Matter, Phys. Rev. D **89**, 076005 (2014).
[38] M. Cirelli, N. Fornengo, M. Taoso, and A. Vittino, Antihelium from dark matter annihilations, J. High Energy Phys. 08 (2014) 009.
[39] V. Poulin, P. Salati, I. Cholis, M. Kamionkowski, and Joseph Silk, Where do the AMS-02 anti-helium events come from? Phys. Rev. D **99**, 023016 (2019).
[40] T. Aramaki, C. J. Hailey, S. E. Boggs, P. von Doetinchem, H. Fuke, S. I. Mognet, R. A. Ong, K. Perez, and J. Zweerink (GAPS Collaboration), Antideuteron sensitivity for the GAPS Experiment, Astropart. Phys. **74**, 6 (2016).
[41] K. Blum, K. C. Yu Ng, R. Sato, and M. Takimoto, Cosmic rays, antihelium, and an old navy spotlight, Phys. Rev. D **96**, 103021 (2017).
[42] M. Korsmeier, F. Donato, and N. Fornengo, Prospects to verify a possible dark matter hint in cosmic antiprotons with antideuterons and antihelium, Phys. Rev. D **97**, 103011 (2018).
[43] Y.-C. Ding, N. Li, C.-C. Wei, Y.-L. Wu, and Y.-F. Zhou, Prospects of detecting dark matter through cosmic-ray antihelium with the antiproton constraints, J. Cosmol. Astropart. Phys. 06 (2019) 004.
[44] I. Cholis, D. Hooper, and T. Linden, A predictive analytic model for the solar modulation of cosmic rays, Phys. Rev. D **93**, 043016 (2016).
[45] I. Cholis, D. Hooper, and T. Linden, Possible evidence for the stochastic acceleration of secondary antiprotons by supernova remnants, Phys. Rev. D **95**, 123007 (2017).
[46] J. F. Navarro, C. S. Frenk, and S. D. M. White, The structure of cold dark matter halos, Astrophys. J. **462**, 563 (1996).
[47] R. Catena and P. Ullio, A novel determination of the local dark matter density, J. Cosmol. Astropart. Phys. 08 (2010) 004.
[48] P. Salucci, F. Nesti, G. Gentile, and C. F. Martins, The dark matter density at the Sun's location, Astron. Astrophys. **523**, A83 (2010).
[49] P. Chardonnet, J. Orloff, and P. Salati, The Production of antimatter in our galaxy, Phys. Lett. B **409**, 313 (1997).
[50] http://galprop.stanford.edu.
[51] A. W. Strong and I. V. Moskalenko, Propagation of cosmic-ray nucleons in the Galaxy, Astrophys. J. **509**, 212 (1998).
[52] R. Trotta, G. Johannesson, I. V. Moskalenko, T. A. Porter, R. Ruiz de Austri, and A. W. Strong, Constraints on cosmic-ray propagation models from a global Bayesian analysis, Astrophys. J. **729**, 106 (2011).
[53] E. S. Seo and V. S. Ptuskin, Stochastic reacceleration of cosmic rays in the interstellar medium, Astrophys. J. **431**, 705 (1994).
[54] http://www.srl.caltech.edu/ACE/ASC/.
[55] http://wso.stanford.edu/Tilts.html.
[56] A. Cuoco, J. Heisig, M. Korsmeier, and M. Krämer, Probing dark matter annihilation in the Galaxy with antiprotons and gamma rays, J. Cosmol. Astropart. Phys. 10 (2017) 053.
[57] T. Aramaki *et al.*, Review of the theoretical and experimental status of dark matter identification with cosmic-ray antideuterons, Phys. Rep. **618**, 1 (2016),
[58] A. Kounine (AMS Collaboration), *Proceedings, 32nd ICRC 2011* (International Union of Pure and Applied Physics, 2011), Vol. 5.
[59] A. Albert *et al.* (DES and Fermi-LAT Collaboration), Searching for dark matter annihilation in recently discovered milky way satellites with Fermi-LAT, Astrophys. J. **834**, 110 (2017).
[60] N. Aghanim *et al.* (Planck Collaboration), Planck 2018 results. VI. Cosmological parameters, Astron. Astrophys. **641**, A6 (2020).
[61] S. Schael *et al.* (ALEPH Collaboration), Deuteron and antideuteron production in e^+e^- collisions at the Z resonance, Phys. Lett. B **639**, 192 (2006).
[62] L. O'C. Drury and A. W. Strong, Power requirements for cosmic ray propagation models involving diffusive reacceleration; estimates and implications for the damping of interstellar turbulence, Astron. Astrophys. **597**, A117 (2017).
[63] E. Orlando and A. Strong, Galactic synchrotron emission with cosmic ray propagation models, Mon. Not. R. Astron. Soc. **436**, 2127 (2013).
[64] G. Di Bernardo, C. Evoli, D. Gaggero, D. Grasso, and L. Maccione, Cosmic ray electrons, positrons and the synchrotron emission of the Galaxy: Consistent analysis and implications, J. Cosmol. Astropart. Phys. 03 (2013) 036.
[65] E. Orlando, Imprints of cosmic rays in multifrequency observations of the interstellar emission, Mon. Not. R. Astron. Soc. **475**, 2724 (2018).
[66] M. Cirelli, G. Corcella, A. Hektor, G. Hutsi, M. Kadastik, P. Panci, M. Raidal, F. Sala, and A. Strumia, PPPC 4 DM ID: A poor particle physicist cookbook for dark matter indirect detection, J. Cosmol. Astropart. Phys. 03 (2011) 051; Erratum, J. Cosmol. Astropart. Phys. 10 (2012) 01.
[67] T. Sjostrand, S. Mrenna, and P. Z. Skands, A Brief Introduction to PYTHIA8.1, Comput. Phys. Commun. **178**, 852 (2008).
[68] G. Corcella, I. G. Knowles, G. Marchesini, S. Moretti, K. Odagiri, P. Richardson, M. H. Seymour, and B. R. Webber, HERWIG6: An event generator for hadron emission reactions with interfering gluons (including supersymmetric processes), J. High Energy Phys. 01 (2001) 010.
[69] P. Meade, M. Papucci, and T. Volansky, Dark matter sees the light, J. High Energy Phys. 12 (2009) 052.
[70] M. Kadastik, M. Raidal, and A. Strumia, Enhanced antideuteron Dark Matter signal and the implications of PAMELA, Phys. Lett. B **683**, 248 (2010).
[71] S. Acharya *et al.* (ALICE Collaboration), Production of deuterons, tritons, ^{3}He nuclei and their antinuclei in pp collisions at $\sqrt{s} = 0.9$, 2.76 and 7 TeV, Phys. Rev. C **97**, 024615 (2018).
[72] L. C. Tan and L. K. Ng, Calculation of the equilibrium antiproton spectrum, J. Phys. G **9**, 227 (1983).
[73] A. Lowell, T. Aramaki, and R. Bird (GAPS Collaboration), An indirect dark matter search using cosmic-ray antiparticles with GAPS, Proc. Sci., ICHEP2018 (**2019**) 543 [arXiv:1812.04800].